

Secret interactions of neutrinos with light gauge boson at the DUNE near detector

P. Bakhti,^{*} Y. Farzan,[†] and M. Rajaei[‡]

School of physics, Institute for Research in Fundamental Sciences (IPM)

P.O.Box 19395-5531, Tehran, Iran

(Dated: October 11, 2018)

Secret interactions of neutrinos with light new gauge bosons, Z' , can lead to a rich phenomenology in supernova explosion as well as in the early universe. This interaction can also lead to new decay modes for charged mesons, $\pi^+(K^+) \rightarrow e^+\nu Z'$ and subsequently to $Z' \rightarrow \nu\bar{\nu}$. After demonstrating that such interaction can be accommodated within viable electroweak symmetric models, we study how the Near Detector (ND) of DUNE can probe this scenario. We also discuss how DUNE ND can make it possible to reconstruct the flavor structure of the Z' coupling to neutrinos.

^{*} pouya_bakhti@ipm.ir

[†] yasaman@theory.ipm.ac.ir

[‡] meshkat.rajaee@ipm.ir

I. INTRODUCTION

The state-of-the-art DUNE experiment which is mainly proposed to measure the CP-violating phase in the lepton sector, is a long baseline setup with two detectors. The Far Detector (FD) will be located at a distance of 1300 km from the source at Sanford Underground Research Facility (SURF). The Near Detector (ND) will be at the site of FermiLAB with a distance of ~ 570 m from the source. Having superb particle recognition and energy-momentum measurement precision and receiving a high flux of neutrinos from the source make the near detector an ideal site to search for new light particles coupled to leptons. For example, Ref. [1] shows that ND of DUNE can be sensitive to MeV range sterile neutrinos that mix with ν_μ and/or ν_e . Refs. [2] discuss the possibility of probing light dark matter particles produced at source via a new gauge interaction involving baryons as well as dark matter particles.

In the present paper, we study the scenario in which neutrinos couple to a light gauge boson Z' with mass smaller than ~ 100 MeV. The new gauge boson can be produced via $\pi^+ \rightarrow l^+ \nu Z'$ or via $K^+ \rightarrow l^+ \nu Z'$ (where $l^+ = e^+$ or μ^+) and subsequently decay into a pair of neutrino and anti-neutrino before reaching the near detector. The produced neutrinos can be detected in ND providing us with information on the intermediate Z' .

Scenarios in which a light gauge boson couples to neutrinos are motivated within various contexts. For example, as shown in [3], it can help to solve the missing satellite problem that is considered a drawback for the canonical cold dark matter scenarios. As demonstrated in [4, 5], such interaction can lead to non-trivial features in propagation of neutrinos within supernova and as a result affect their energy spectrum. If such a coupling exists in nature but we overlook them in analyzing supernova or cosmological data, we will be lead to wrong conclusion. It is therefore imperative to probe the possible new couplings of neutrinos by terrestrial experiments as much as we can. If the Z' also couples to matter fields, its effect can be probed by scattering experiments [6] or by its impact on neutrino oscillation in matter. However, if the only standard particles that couple to Z' are neutrinos, these experiments will not be able to test the scenario.

From model building point of view, it is straightforward to build a model giving rise to this scenario. As shown in [7, 8], if there is a sterile neutrino that is charged under a new $U(1)$ gauge symmetry and is mixed with active neutrinos, the active neutrinos will also obtain a coupling to the gauge boson of the new $U(1)$ gauge symmetry. For completeness, we will outline the features of these models and discuss when the sterile neutrinos can be integrated out.

As shown in [9], the meson decay experiments such as NA62 and PIENU can also search for such Z' . In these experiments, the charged lepton produced in decay of the charged meson can be identified but the prompt neutrino, as well as the neutrino anti-neutrino pair produced in the decay of Z' go undetected. As a result, these meson decay experiments are sensitive to $\sum_{\alpha \in \{e, \mu, \tau, [s]\}} |g_{e\alpha}|^2$ and $\sum_{\alpha \in \{e, \mu, \tau, [s]\}} |g_{\mu\alpha}|^2$ [in which ν_s is a possible sterile neutrino which couples to Z' along with ν_μ or ν_e and is lighter than the decaying meson]. On the other hand, the charged lepton at the source of DUNE will not be detected but instead, the produced neutrino can be detected at ND providing complementary information on the flavor structure of Z' coupling.

The present paper is organized as follows. In sect II, we describe two classes of $U(1)$ gauge models that give rise to neutrino interaction with Z' . In sect III, we compute the spectrum of neutrinos from $\pi^+ \rightarrow l^+ \nu Z'$ and subsequent $Z' \rightarrow \nu \bar{\nu}$ in the lab frame. In sec IV, constraints on the coupling of Z' with neutrinos are discussed using DUNE near detector. Section V is devoted to summary and discussion.

II. MODELS FOR NEUTRINO INTERACTIONS WITH NEW LIGHT GAUGE BOSON

In this section, we briefly review two classes of models that give rise to interactions of type

$$\sum_{\alpha, \beta} g_{\alpha\beta} Z'_\mu \bar{\nu}_\alpha \gamma^\mu \nu_\beta. \quad (1)$$

As is well-known such interaction can come from gauging various combination of lepton flavors and baryon number $a_e L_e + a_\mu L_\mu + a_\tau L_\tau + bB$ where a_e, a_μ, a_τ and b are arbitrary real numbers that satisfy the anomaly cancellation condition $a_e + a_\mu + a_\tau + 3b = 0$. For such gauge interaction, $g_{\alpha\alpha} \propto a_\alpha$ and $g_{\alpha\beta}|_{\alpha \neq \beta} = 0$. Famous combinations which have been extensively studied in the literature are $B - L = B - L_e - L_\mu - L_\tau$, $L_\mu - L_\tau$, $L_e - L_\tau$ and $L_\mu - L_e$. Notice that in these models, along with neutrinos, the corresponding charged leptons also couple to Z' . There are strong bounds on the coupling of the electron to Z' from various observations across a wide range of Z' mass. Because of the strong bounds on the electron coupling to Z' , we will not emphasize on this class of models any further.

We now discuss another possibility for model building which was proposed in [7, 8]. Let us introduce a Dirac fermion Ψ charged under the new $U(1)$ and mixed with ν_α . Denoting the gauge coupling by g_Ψ , the gauge interaction term is $g_\Psi Z'_\mu \bar{\Psi} \gamma^\mu \Psi$. Since Ψ mixes with active neutrinos, the active neutrinos of flavor ν_α will be a linear combination

of mass eigenstates ν_i :

$$\nu_\alpha = \sum_{i=1}^4 U_{\alpha i} \nu_i \quad (2)$$

in which ν_4 is the heavier state that gives the main contribution to Ψ ; *i.e.*, $U_{\Psi 4} \simeq 1$, $U_{\alpha 4}|_{\alpha=e,\mu,\tau} \ll 1$. Since ν_4 is taken to be heavier than the charged meson, M^+ , in decay $M^+ \rightarrow l_\alpha^+ \nu + X$ (where X can be any state), the coherent ν state will not exactly be ν_α (as defined in Eq. 2) but will coincide with a linear combination of ν_1 , ν_2 and ν_3 which cannot be perpendicular to Ψ . In particular, for $M^+ \rightarrow l_\alpha^+ \nu$, it will be $\sum_{i=1}^3 U_{\alpha i} \nu_i$ so $\langle \Psi | \sum_{i=1}^3 U_{\alpha i} \nu_i \rangle = -U_{\Psi 4}^* U_{\alpha 4}$. Integrating out the heavy 4th state, the light active neutrinos receive a coupling of form¹

$$g_{\beta\alpha} Z'_\mu \bar{\nu}_\beta \gamma^\mu \nu_\alpha$$

in which

$$g_{\beta\alpha} = g_\Psi |U_{\Psi 4}|^2 U_{\alpha 4} U_{\beta 4}^* \simeq g_\Psi U_{\alpha 4} U_{\beta 4}^*.$$

As a result, three body decays such as π^+ (or K^+) $\rightarrow l_\alpha^+ \nu_\beta Z'$ can take place with a rate proportional to $|g_{\alpha\beta}|^2$. Z' will subsequently decay into $\bar{\nu}_\alpha \nu_\beta$ again with a rate proportional to $|g_{\alpha\beta}|^2$. However if ν_4 is lighter than the parent charged lepton, we cannot integrate it out and the picture will be different. In this case, the neutrino state produced at charged meson decay via SM interactions will be $\nu_\alpha = \sum_{i=1}^4 U_{\alpha i} \nu_i$ but if ν_4 is heavy enough, it will decohere from ν_1 , ν_2 and ν_3 , giving rise to Ψ production given by $|U_{\alpha 4}|^2 |U_{\Psi 4}|^2 \simeq |U_{\alpha 4}|^2$ but this is not the case we are interested in here. For our case with $m_\Psi \sim 1$ GeV, $W^+ \rightarrow l_\alpha^+ \nu_\alpha$ will take place with a rate deviated from the standard model prediction by a small amount of $O[|U_{\alpha 4}|^2 (m_\Psi^2/m_W^2)] \ll 1$. The ν_4 component in ν_α will subsequently decay into $\nu_i|_{i<4}$ and Z' which appears again as missing energy at colliders.

As discussed in Ref [8], there are at least two mechanisms for mixing Ψ with ν_α . In one method which is described in detail in [7], a new Higgs doublet H' charged under the new $U(1)$ is introduced such that its VEV induces a mixing between Ψ and ν_α via Yukawa coupling of the form $\bar{L}_\alpha H'^T c \Psi$. In the other model described in detail in sect IV.B of [8], no new Higgs doublet is required. Instead, a neutral Dirac N and a new scalar singlet, S charged under $U(1)$ are introduced with interaction terms similar to that in the inverse seesaw mechanism: $Y_\alpha \bar{N}_R H^T c L_\alpha + \lambda_L S \bar{\Psi}_R N_L$. The mixing $U_{\alpha 4}$ will be given by $Y_\alpha \langle H \rangle \lambda_L \langle S \rangle / (m_N m_\Psi)$.

Notice that in this class of models at tree level only neutrinos couple to Z' so they are free from the bounds on the coupling of the corresponding charged leptons to Z' . In general, we expect $|g_{\alpha\beta}| = |g_{\beta\alpha}|$. Depending on the sign of g_Ψ , $g_{\alpha\alpha}$ can be either positive or negative. If there is only one Ψ mixed with ν_α and ν_β , we expect $|g_{\alpha\beta}|^2 = |g_{\alpha\alpha}|^2 |g_{\beta\beta}|^2$ and if there are more than one Ψ , the Schwartz inequality implies $|g_{\alpha\beta}|^2 < |g_{\alpha\alpha}|^2 |g_{\beta\beta}|^2$. There are strong bounds on the deviation of the 3×3 PMNS mixing matrix from the unitarity that can be translated into the bounds on $g_{\alpha\beta}$ [7]. In this paper, we are mainly interested in the g_{ee} and $g_{e\tau}$ elements because they can lead to kinematically favored decay modes $\pi^+ \rightarrow e^+ \nu_e Z'$ and $\pi^+ \rightarrow e^+ \nu_\tau Z'$, respectively. To obtain nonzero g_{ee} , it is enough to mix Ψ only with ν_e . For gauge coupling in the perturbative range (*e.g.*, $g_\Psi \lesssim 4$) the bound from unitarity (*i.e.*, $|U_{e4}|^2 < 2.5 \times 10^{-3}$ [10]) leads to $g_{ee} \lesssim 10^{-2}$. Notice that in this case, we are not introducing a new source of Lepton Flavor Violating (LFV) so no strong bound comes from $\mu \rightarrow e \gamma$ and from similar LFV processes. The unitarity bound on $|U_{e4} U_{\tau 4}^*|$ is 3.7×10^{-3} [10] which again translates into $g_{e\tau} \lesssim 10^{-2}$. As discussed in [7], the LFV process $\tau \rightarrow e \gamma$ is GIM suppressed and does not yield a strong bound.

III. FLUX OF NEUTRINOS FROM PION DECAY INTO Z'

In this section, we compute the flux of neutrinos from pion decay, $\pi^+ \rightarrow Z' \nu l_\alpha^+$ as well as from subsequent Z' decay $Z' \rightarrow \nu \bar{\nu}$. Similar formulas hold valid for $K^+ \rightarrow Z' \nu l_\alpha^+$ with replacing $f_\pi \rightarrow f_K$, $m_\pi \rightarrow m_K$ and $\cos \theta_C \rightarrow \sin \theta_C$. In general, we can write the flux of neutrinos in the lab frame, $\phi(E_\nu)$ as

$$\phi(E_\nu) = \frac{1}{4\pi L^2} \int_{E_\pi^{min}}^{E_\pi^{max}} dE_\pi P_\pi(E_\pi) \left(\frac{dN_\nu}{dE_\nu} \right)_{lab} \frac{d\Omega_{r.\pi}}{d\Omega_{lab}}, \quad (3)$$

¹ In [7], $U_{\alpha 4}$ was denoted by κ_α .

where L is the distance from the source to the detector and $P_\pi(E_\pi)$ is the rate of the pion injection in the lab frame. $(\frac{dN_\nu}{dE_\nu})_{lab}$ is the spectrum of the neutrino in the lab frame from decay of a pion with energy of E_π and is related to the spectrum of neutrinos in the rest frame of pion, $dN_\nu/dE_\nu|_{r,\pi}$, as

$$(\frac{dN_\nu}{dE_\nu})_{lab} = (\frac{dN_\nu}{dE_\nu})|_{r,\pi} \frac{\partial E_\nu|_{r,\pi}}{\partial E_\nu|_{lab}}. \quad (4)$$

Setting the angle between the direction of neutrinos reaching the detector and the momentum of pion beam zero², we can write $E_\nu|_{lab} = E_\nu|_{r,\pi}(1 + v_\pi)\gamma_\pi$ in which v_π is the pion velocity in the lab frame and $\gamma_\pi = (1 - v_\pi^2)^{-1/2}$. Thus,

$$\frac{\partial E_\nu|_{r,\pi}}{\partial E_\nu|_{lab}} = \gamma_\pi(1 - v_\pi).$$

Finally $d\Omega_{r,\pi}/d\Omega_{lab} = (1 + v_\pi)/(4(1 - v_\pi)) \simeq \gamma_\pi^2$ takes care of focusing of the beam in the direction of the detector.

In the following, we compute the spectrum of neutrinos from $\pi \rightarrow e\nu_\alpha Z'$ and $Z' \rightarrow \nu\bar{\nu}$, neglecting the mass of the electron. We return to the case of $\pi \rightarrow \mu\nu Z'$ in the end of this section. It is straightforward to show that the spectrum of the prompt ν in the rest frame of the pion is given by

$$\frac{d\Gamma(\pi \rightarrow e\nu_\alpha Z')}{dE_\nu}|_{r,\pi} = \frac{f_\pi^2 g_{e\alpha}^2 G_F^2 \cos^2(\theta_C)}{64\pi^3 m_\pi^2 m_{Z'}^2 (m_\pi - 2E_\nu)^2} E_\nu^2 (2E_\nu m_\pi - m_\pi^2 + m_{Z'}^2)^2 (-2E_\nu m_\pi + m_\pi^2 + 2m_{Z'}^2). \quad (5)$$

Computing the spectrum of neutrinos for Z' decay in the rest frame of pion is slightly more complicated. The energies of ν and $\bar{\nu}$ in the rest frame of Z' are equal to $m_{Z'}/2$ but their energies in the rest frame of the pion depend on the angle between the direction of their emission and the direction of the Z' momentum. Moreover, the angular distribution of neutrino and antineutrino (even in the rest frame of Z') depends on the polarization of Z' . We therefore have to make computation for each Z' polarization separately.

In the rest frame of the pion, the differential decay rate of the pion to the electron, neutrino and Z' with polarization perpendicular to the Z' momentum (ϵ_1, ϵ_2) and parallel (ϵ_3) to the Z' momentum are respectively

$$\frac{d\Gamma(\pi \rightarrow e\nu_\alpha Z')}{dE_{Z'}}|_{1,2} = \frac{f_\pi^2 g_{e\alpha}^2 G_F^2 \cos^2(\theta_C)}{96\pi^3 m_\pi} p_{Z'} (-2E_{Z'} m_\pi + m_\pi^2 + m_{Z'}^2) \quad (6)$$

and

$$\frac{d\Gamma(\pi \rightarrow e\nu_\alpha Z')}{dE_{Z'}}|_3 = \frac{f_\pi^2 g_{e\alpha}^2 G_F^2 \cos^2(\theta_C)}{96\pi^3 m_\pi m_{Z'}^2} p_{Z'} (E_{Z'} m_\pi - m_{Z'}^2)^2. \quad (7)$$

Notice that as expected, the decay into longitudinal mode is proportional to $g_{e\alpha}^2/m_{Z'}^2$ and will be enhanced for $m_{Z'} \ll m_\pi$.

The total decay rate of the $Z' \rightarrow \nu_\alpha \bar{\nu}_\beta$ for all the polarizations are equal to

$$\Gamma(Z' \rightarrow \nu_\alpha \bar{\nu}_\beta) = \frac{g_{\alpha\beta}^2 m_{Z'}}{24\pi}.$$

The conditions for Z' decay before reaching the near and far detectors of DUNE ($\Gamma(m_{Z'}/E_{Z'})L > 1$) are respectively $g_{\alpha\beta} > 2 \times 10^{-7} (10 \text{ MeV}/m_{Z'})$ and $g_{\alpha\beta} > 4 \times 10^{-9} (10 \text{ MeV}/m_{Z'})$.

The neutrino spectrum produced from Z' decay with polarization i in the rest frame of Z' is given by

$$(\frac{dN_\nu}{d\Omega})_{r,Z'}|_i = \frac{1}{\Gamma(Z' \rightarrow \nu\bar{\nu})} \frac{d\Gamma(Z' \rightarrow \nu\bar{\nu})}{d\Omega}|_i, \quad (8)$$

For ϵ_1 and ϵ_2 , the normalized spectrum is

$$(\frac{dN_\nu}{d\cos\theta})_{r,Z'}|_{1,2} = \frac{3(1 + \cos^2\theta)}{8}, \quad (9)$$

² Remember that the DUNE setup is going to be on-axis and the angle subtending the ND is $\sim O(3.5 \text{ m}/570 \text{ m})$.

and in the case of ϵ_3 is

$$\left(\frac{dN_\nu}{d\cos\theta}\right)_{r,Z'}|_3 = \frac{3\sin^2\theta}{4}, \quad (10)$$

where θ is the angle between the direction of the neutrino in the rest frame Z' and the direction of Z' emission in the rest frame of the pion. As expected $\sum_{i=1}^3 (dN_\nu/d\cos\theta)_{r,Z'}$ is independent of θ . From Eqs. (9,10), we observe that the angular distribution is invariant under $\theta \rightarrow \pi - \theta$ which means that the neutrinos and antineutrinos from the Z' decay have the same angular distribution. This is rather counter-intuitive because angular momentum conservation combined with the fact that (anti)neutrinos are (right-)left-handed implies that if the spin of Z' is in *e.g.*, the state of $|l=1, m=+1\rangle$, antineutrinos (neutrinos) will be emitted parallel (anti-parallel) to the spin direction. Notice however that none of the 1, 2 and 3 polarization corresponds to $|l=1, m=+1\rangle$ or $|l=1, m=-1\rangle$. In fact, the 3 polarization corresponds to $|l=1, m=0\rangle$ and the 1 and 2 polarizations are linear combinations of $|l=1, m=\pm 1\rangle$. Thus, angular momentum conservation implies that the decays of each of these polarizations lead to the emission of both parallel and antiparallel neutrinos and antineutrinos as reflected in Eqs (9,10). Remembering that the energy of ν (or $\bar{\nu}$) in the rest frame of Z' is $m_{Z'}/2$, its energy in the pion rest frame will be

$$E_\nu|_{r,\pi} = \frac{m_{Z'}}{2} \gamma_{Z'} (1 + v_{Z'} \cos\theta) \quad (11)$$

in which $v_{Z'}$ is the velocity of the Z' in the rest frame of pion, $v_{Z'} = (1 - m_{Z'}^2/E_{Z'}^2)^{1/2}$ and $\gamma_{Z'} = (1 - v_{Z'}^2)^{-1/2}$. In the rest frame of pion, the spectrum of neutrino produced from Z' decay is then

$$\left(\frac{dN_\nu}{dE_\nu}\right)_{r,\pi}|_i = \left(\frac{dN_\nu}{d\cos\theta}\right)_{r,Z'}|_i \frac{d\cos\theta|_{r,Z'}}{dE_\nu|_{r,\pi}} = \left(\frac{dN_\nu}{d\cos\theta}\right)_{r,Z'}|_i \frac{2}{E_{Z'} v_{Z'}}. \quad (12)$$

We already noticed that $(dN_\nu/d\cos\theta)_{r,Z'} = (dN_{\bar{\nu}}/d\cos\theta)_{r,Z'}$ so in the rest frame of the pion, the energy spectrum of neutrinos and antineutrinos from Z' decay will be the same. The total neutrino spectrum from Z' decay in the rest frame of pion is given by

$$\left(\frac{dN_\nu}{dE_\nu}\right)_{r,\pi}^{Z' \text{ decay}} = \sum_i \int_{E_{Z'}^{min}}^{E_{Z'}^{max}} dE_{Z'} \frac{dN_{Z'}}{dE_{Z'}}|_i \left(\frac{dN_\nu}{dE_\nu}\right)_{r,\pi}|_i \quad (13)$$

in which i refers to the Z' polarization, $E_{Z'}^{min} = E_\nu + m_{Z'}^2/(4E_\nu)$, $E_{Z'}^{max} = (m_\pi^2 + m_{Z'}^2)/(2m_\pi)$ and

$$\frac{dN_{Z'}}{dE_{Z'}}|_i = \frac{1}{\Gamma_{total}^\pi} \frac{d\Gamma(\pi \rightarrow e\nu Z')}{dE_{Z'}}|_i. \quad (14)$$

Similar consideration holds for the decay $\pi^+ \rightarrow \mu^+ Z' \nu$ with the difference that the mass of μ^+ cannot be neglected. To avoid cluttering, we will not show the formulas here. Notice however that because of phase space, the decay into muon is significantly suppressed. In fact for $m_{Z'} > 5$ MeV, $\Gamma(\pi \rightarrow \mu\nu_\alpha Z')/\Gamma(\pi \rightarrow e\nu_\alpha Z')$ is smaller than $0.055|g_{\mu\alpha}|^2/|g_{e\alpha}|^2$ and reaches $< 0.01|g_{\mu\alpha}|^2/|g_{e\alpha}|^2$ from $m_{Z'} > 20$ MeV.

IV. LIGHT Z' AND THE DUNE NEAR DETECTOR

In this section, we discuss how the data from the DUNE near detector can be used to extract information on the coupling of neutrinos to Z' . To compute the flux of neutrinos from new pion and kaon decay mode, we have used the formalism developed in section III. The energy spectra of the charged pion and kaon are demonstrated in Fig. 1 [11] which correspond to the 120 GeV mode and the total number of all particles equal to 1.396×10^6 . Fig. 2 shows the predicted flux of neutrinos of different flavors from the π^+ decay within the SM [12] and compares it with the ν_e and $\bar{\nu}_e$ spectra from new physics with Z' of 10 MeV mass and coupling of $g_{ee} = 0.1$. Such a large value of g_{ee} is already ruled out but we have chosen this value for illustrative purposes. For smaller values of g_{ee} , the flux will be just scaled by g_{ee}^2 . The cyan curve shows the electron anti-neutrino spectrum coming from Z' decay. The magenta curve shows the electron neutrino spectrum coming from both Z' and π^+ decays. Remembering that ν and $\bar{\nu}$ from the Z' decay have the same energy spectrum, the difference between purple and cyan curves gives the spectrum of neutrinos produced from the pion decay, $\pi^+ \rightarrow e^+ Z' \nu$.

To compute the number of events, we have taken the neutrino cross section from Ref. [13, 14]. For the analysis, we consider ten years of the data taking with 1.5×10^{21} POT/year in π^+ decay mode, for neutrinos with the energies from 1 GeV to 30 GeV, dividing to 29 equal size bins. In fact, DUNE will operate both in the π^+ and π^- modes.

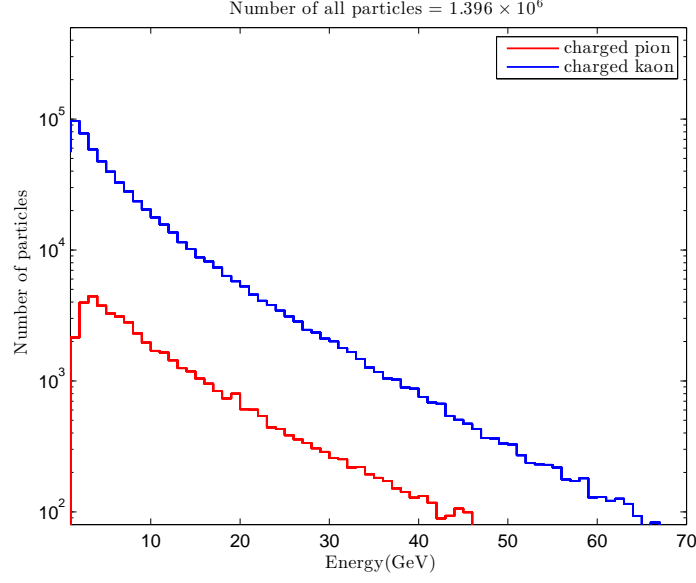


FIG. 1. The spectrum of charged pion and kaon in the beginning of the decay pipe in the DUNE experiment, taking the total number of all particles equal to $= 1.396 \times 10^6$ [11].

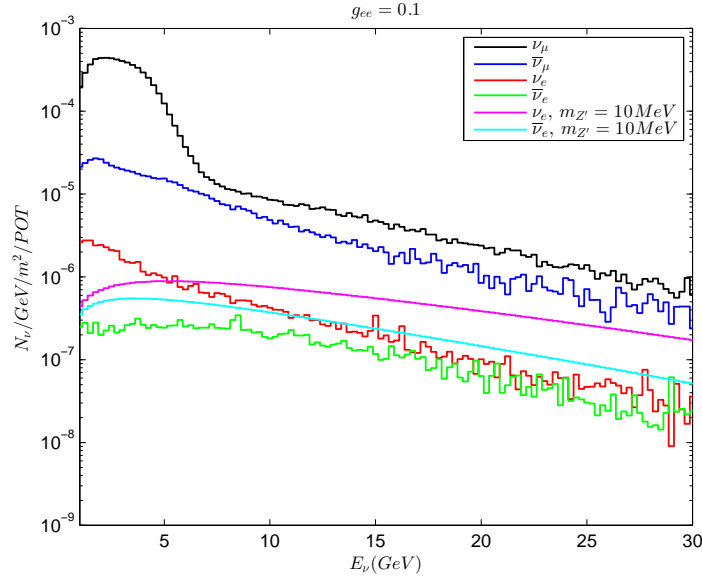


FIG. 2. Fluxes of neutrinos at the near detector of DUNE for different flavors within the standard model [12] in the π^+ mode. The ν_e and $\bar{\nu}_e$ fluxes from new physics with $g_{ee} = 0.1$ and $m_{Z'} = 10$ MeV are also shown with magenta and cyan lines, respectively.

We repeated the analysis for such program, taking the π^+ and K^+ energy spectra in the π^+ mode equal to the π^- and K^- energy spectra in the π^- mode. The overall results were unchanged. In fact, our signals are CP invariant and we expect the antineutrino flux of a given flavor from π^+ or K^+ decay to be equal to that from the π^- or K^- decay. The small difference between two modes comes only from the difference between cross sections of neutrinos and antineutrinos at the detector. For simplicity in our analysis, we consider perfect energy resolution and efficiencies or acceptance for the ν_e and $\bar{\nu}_e$ at the DUNE near detector. In fact, we repeated the analysis with setting the efficiencies of the ν_e and ν_μ detection to 80% and 85% [15], respectively and simultaneously increasing the total flux with a factor

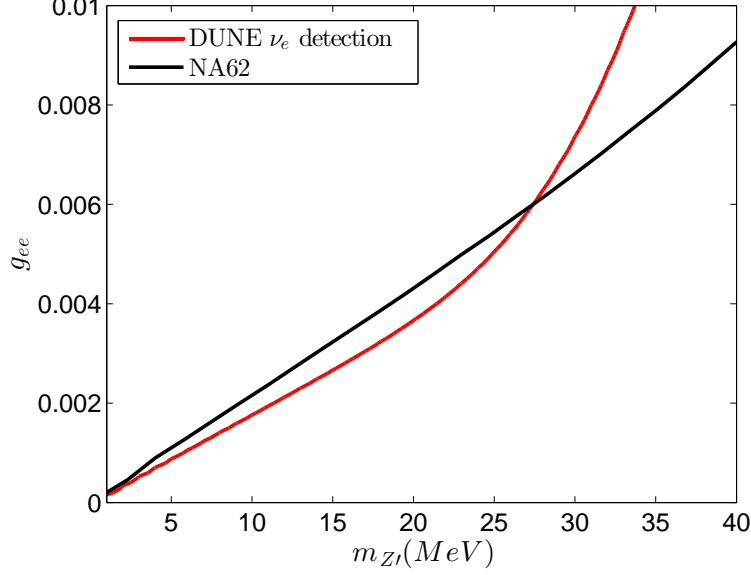


FIG. 3. The upper bound on g_{ee} vs. $m_{Z'}$ at 90% C.L. The red curve shows the DUNE constraint on g_{ee} by ν_e detection after ten years of data taking with 1.5×10^{21} POT/year in the π^+ mode. The black line shows the NA62 current constraint on g_{ee} [9].

of 1.25. We then found that the results are unchanged. The near detector of DUNE will measure the absolute flux to 2.5% precision, via neutrino-electron scattering [16]. For statistical inference, we have used the chi-squared method defined as

$$\chi^2 = \sum_{bins} \frac{[N_{th}^i(1 + \eta) - N_{exp}^i]^2}{\sigma_i^2} + \frac{\eta^2}{(\Delta\eta)^2}, \quad (15)$$

in which N_{th}^i is the theoretical prediction for the number of events in each bin, assuming a certain value of $g_{e\alpha}$ and $m_{Z'}$. N_{exp}^i is the forecast for median number of events in each, assuming a certain true value for $m_{Z'}$ and coupling. η is the nuisance parameter that takes care of the normalization uncertainty of $\Delta\eta = 2.5\%$. The details of the near detector are under discussion, however, we assume a 84 ton fiducial mass of LArTPC detector and multi-purpose tracker TBD at 575 m from the source.

Fig. 3 shows the 90% C.L. constraints on the g_{ee} versus $m_{Z'}$ setting all the true values $g_{\alpha\beta} = 0$. We have considered neutrinos both from kaon and pion decay. The best current constraint on $\sqrt{\sum_{\alpha} g_{e\alpha}^2}$ which comes from the Kaon decay measurement at NA62 experiments [9], is also shown in the Fig. 3. Comparing with current constraints, near detector of DUNE will constrain the coupling stronger for $m_{Z'} < 30$ MeV. Above 30 MeV, the current bound from NA62 is stronger than the reach of DUNE because, while for heavy Z' , $\pi \rightarrow Z'\nu_e$ is suppressed due to the phase space, $m_{Z'}$ is still much lighter than K and therefore $K \rightarrow Z'\nu_e$ is not suppressed. For $m_{Z'} < 25$ MeV, the neutrinos from π^+ at DUNE dominate over those from K^+ . That is for $m_{Z'} < 25$ MeV, even if we neglected the K^+ flux, we would obtain the same bound from DUNE. The contribution from K^+ becomes important only for $m_{Z'} > 30$ MeV where the NA62 bound is stronger. As a result, across the $m_{Z'}$ range that we expect DUNE to improve the NA62 bounds, the results will not suffer from uncertainties in computing the K^+ flux.

As it is explained in the conceptual design of the DUNE [16], both near and far detectors will be sensitive to the detection of ν_τ . In the case of non-zero $g_{e\tau}$, $\bar{\nu}_\tau$ and ν_τ are produced via $\pi^+ \rightarrow e^+ Z' \nu_\tau$ followed by $Z' \rightarrow \nu_e \bar{\nu}_\tau$ and $Z' \rightarrow \bar{\nu}_e \nu_\tau$. Thus, near detector of DUNE has the potential to constrain $g_{e\tau}$ by ν_τ and $\bar{\nu}_\tau$ detection. The charged current interactions of ν_τ ($\bar{\nu}_\tau$) at the detector can lead to τ ($\bar{\tau}$) production. Three decay modes of τ (and $\bar{\tau}$) can be used for reconstructing ν_τ (and $\bar{\nu}_\tau$): (i) $\tau^- \rightarrow e^- \bar{\nu}_e \nu_\tau$ with branching ratio of 17.8%, (ii) $\tau^- \rightarrow \pi^- \nu_\tau (n\pi^0)$ with branching ratio of 49.8% and (iii) $\tau^- \rightarrow \pi^- \pi^+ \pi^- \nu_\tau (n\pi^0)$ with branching ratio of 15.2%. We have only considered hadronic decay channels in our analysis. To our best knowledge, the background for ν_τ and the detection efficiency at DUNE is not still known. To carry out our analysis, we rely on the estimates that have been made for previous setups, keeping in mind that superior particle identification power at DUNE will lead to better estimating the ν_τ detection efficiency and more suppressed background. In Ref. [17] the backgrounds for atmospheric ν_τ are estimated

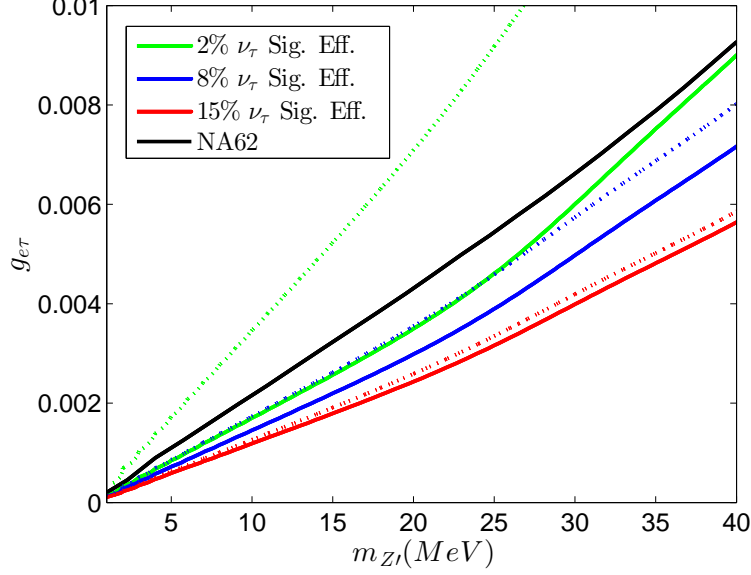


FIG. 4. The upper bound on $g_{e\tau}$ vs. $m_{Z'}$ at 90 % C.L., setting the rest of $g_{\alpha\beta} = 0$. The dashed colored lines show the constraint on $g_{e\tau}$ using only ν_τ and $\bar{\nu}_\tau$ signals with detection efficiencies of 2%, 8% and 15% for 1.5×10^{21} POT/year in the π^+ mode. The corresponding solid lines show the constraints from combining all ν_e , $\bar{\nu}_e$, ν_τ and $\bar{\nu}_\tau$ signals. The black curve shows current bound from NA62 [9].

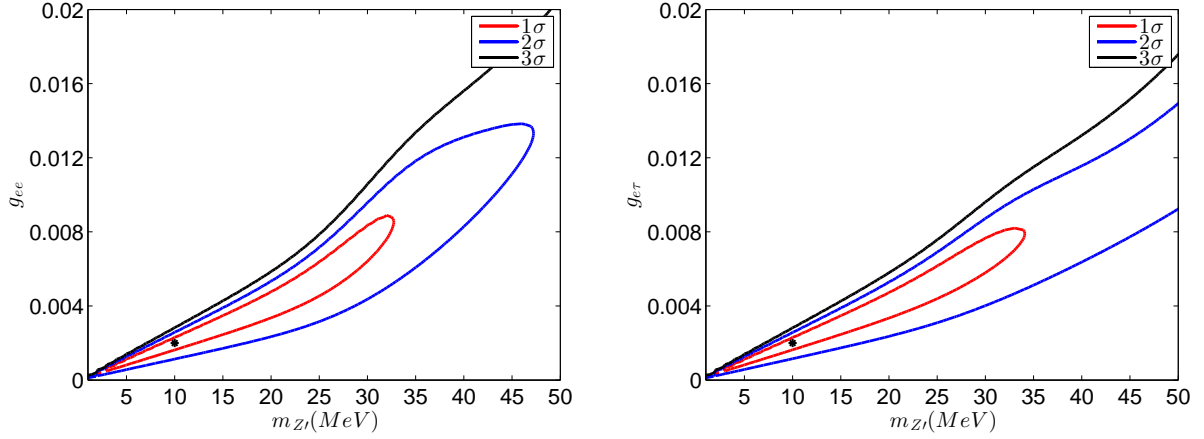


FIG. 5. Discovery potential of near detector of DUNE. The black dot shows the assumed true values for $m_{Z'}$ and g_{ee} in the left panel ($g_{e\tau}$ in the right panel). The contour plots are 1σ , 2σ and 3σ solutions from DUNE near detector after ten years of data taking with 1.5×10^{21} POT/year in the π^+ mode. To extract the value of $g_{e\tau}$ in the right panel we have assumed 8% efficiency and have combined the information from all ν_e , $\bar{\nu}_e$, ν_τ and $\bar{\nu}_\tau$ signals.

for a LAr-TPC detector. Notice that the atmospheric neutrino flux is isotropic. In the beamed experiments such as NOMAD or DUNE, kinematic cuts can help to significantly reduce background. The main source of the background for ν_τ detection via hadronic channel is neutrino neutral-current interaction. Since the efficiency of GeV scale e and μ identification at the LAr neutrino detectors is very high [17], the background from the charged-current interactions of $\nu_\mu/\bar{\nu}_\mu$ and $\nu_e/\bar{\nu}_e$ is negligible for ν_τ detection. In Ref. [18], the backgrounds for ν_τ have been obtained for NOMAD experiment using kinematic cuts on the momenta of $\bar{\nu}_\tau$ and ν_τ . For the strongest kinematic cuts which were designed to reduce background from both neutral current and charged current interactions, the signal efficiency for hadronic mode at NOMAD was 2% [18] and the background rejection for neutral current in hadronic channel was 2×10^{-5} . At DUNE, the kinematic cuts can be less stringent because only neutral currents induce background. In addition, DUNE

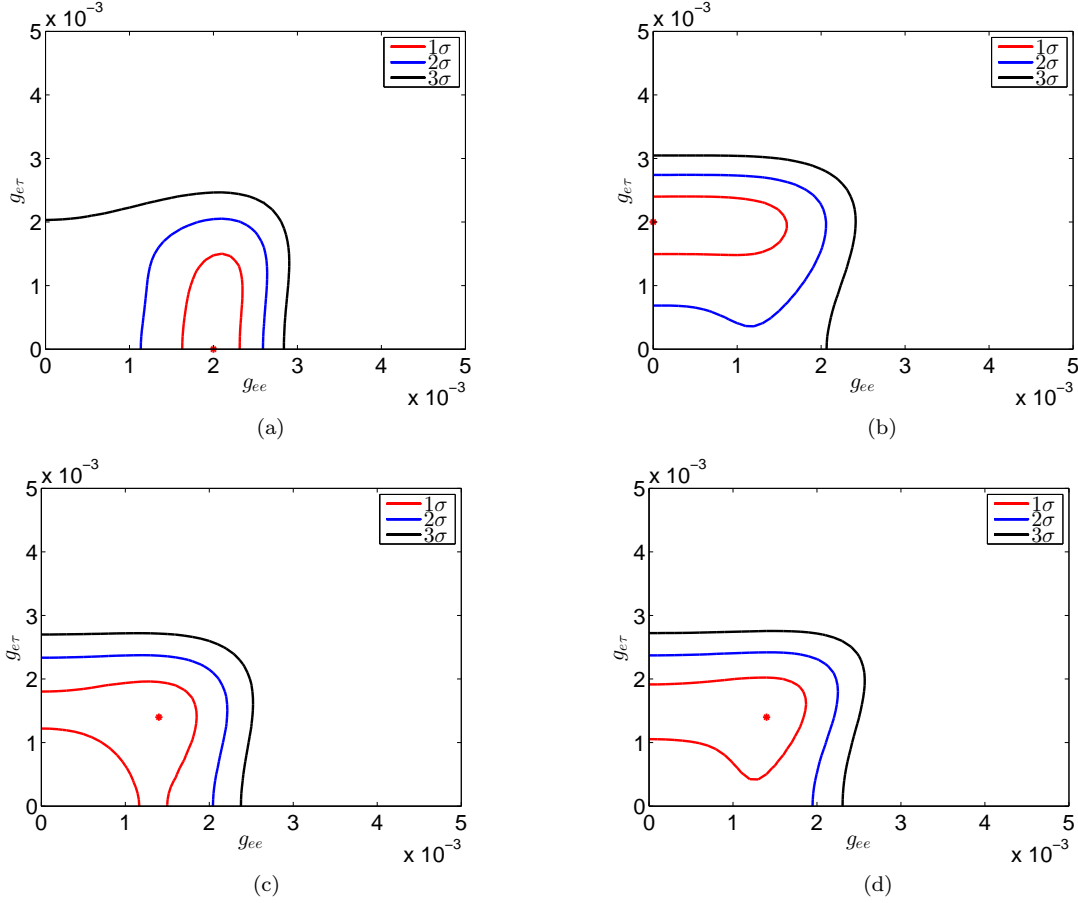


FIG. 6. The capability of DUNE ND in reconstructing the flavor structure of $g_{\alpha\beta}$. The true value of $m_{Z'}$ is taken to be 10 MeV. The red dot in each plot shows the assumed true value of g_{ee} and $g_{e\tau}$. In panels (a,b,c), the rest of coupling components are set to zero but in panel b, we take $g_{\tau\tau} = g_{e\tau}^2/g_{ee}$. The curves show the 1σ , 2σ and 3σ solutions fixing $m_{Z'}$ to 10 MeV after ten years of data taking for 1.5×10^{21} POT/year in the π^+ mode with 8 % ν_τ detection efficiency.

near detector is more sensitive to neutron and pion detection than NOMAD experiment, further enabling reduction of background. In the case of neutron detection, as it is mentioned in the conceptual design of DUNE [16], future experiment CAPTAIN, will be able to determine the response of LAr-TPC to neutrons by higher accuracy. Thus, it is reasonable to take an efficiency for ν_τ detection higher than 2 %. In our analysis, we take an efficiency of 2×10^{-5} in suppressing the background from neutral current events (the same as NOMAD) and we take various values of the ν_τ detection efficiency between 2 % to 15 %. One should however bear in mind that the NC background reduction at DUNE can also be much better than that at NOMAD.

Fig. 4 shows the bound that DUNE ND can set on $g_{e\tau}$ if there is no new physics (*i.e.*, if $g_{\alpha\beta} = 0$) and compares it to the bound from NA62 on $(\sum_\alpha |g_{e\alpha}|^2)^{1/2}$. While to draw the dashed lines, only ν_τ and $\bar{\nu}_\tau$ signals are invoked, to draw the solid lines all the ν_e , $\bar{\nu}_e$, ν_τ and $\bar{\nu}_\tau$ signals are used. The green, blue and red lines respectively correspond to 2 %, 8 % and 15% efficiencies in ν_τ and $\bar{\nu}_\tau$ detection. As seen the bound significantly improves with increasing the detection efficiency. Even with a 2 % efficiency, the combined electron- and tau-neutrino signals lead to a bound on $g_{e\tau}$ stronger than that from NA62.

Fig. 5 shows the discovery potential of DUNE ND assuming that values of couplings are slightly below the current bound from NA62. At each panel only one $g_{\alpha\beta}$ is taken to be nonzero. As seen from the figure, the DUNE can determine the ratio $g_{ee}/m_{Z'}$ or $g_{e\tau}/m_{Z'}$ at 2 σ C.L. For the values of coupling considered, $g_{e\tau} \rightarrow 0$ (at a finite $m_{Z'}$) is ruled out at 2 σ C.L. As seen also at 2 σ C.L., an upper bound on $m_{Z'}$ can be derived but $m_{Z'}, g \rightarrow 0$ (with fixed $g/m_{Z'}$) cannot be ruled out. This is because as $m_{Z'} \rightarrow 0$, the rate of $\pi^+ \rightarrow e^+ \nu Z'$ increases as $g^2/m_{Z'}^2$, without any particular feature in the energy spectrum.

Fig. 6 shows how DUNE ND can reconstruct the flavor structure of the coupling. To draw Fig. 6-a, 6-b and 6-c, only the ee and $e\tau$ components are allowed to be nonzero but to draw Fig. 6-d, we take $g_{\tau\tau} = g_{e\tau}^2/g_{ee}$ as predicted by the model presented in sect. II. The ν_τ detection efficiency is taken to be 8%. As seen from Figs 6-a and 6-b, for the

assumed values of couplings, the DUNE ND can tell us whether the signal comes from nonzero g_{ee} or from nonzero $g_{e\tau}$ at 2σ C.L. This is the great advantage of ND DUNE over the Kaon decay experiments such as NA62 which can only determine $g_{ee}^2 + g_{e\mu}^2 + g_{e\tau}^2$ and originates from the fact that DUNE ND can detect the final neutrino states. Notice that for drawing these figures, we have assumed that we know the true value of $m_{Z'}$. That is in computing χ^2 , we have set $m_{Z'}$ in both N_{exp}^i and N_{th}^i equal to 10 MeV. Of course in reality, $m_{Z'}$ will be unknown. However, the lack of knowledge of $m_{Z'}$ does not ruin the flavor reconstruction power of DUNE ND because it comes from the ratio of the $\nu_\tau + \bar{\nu}_\tau$ signal to the $\nu_e + \bar{\nu}_e$ signal rather than the absolute number of events. We examined this by taking the “true” value of $m_{Z'} = 10$ MeV and the “assumed” value of $m_{Z'}$ in N_{th}^i equal to 25 MeV. As expected the contours turned up to be similar to those shown in Fig. 6 but scaled up by the ratio of the two “true” and “assumed” values of $m_{Z'}$.

Notice that so far only ee and $e\tau$ components are discussed. If only $g_{\tau\tau}$ is nonzero, we do not expect any signal at DUNE ND as $\pi^+ \rightarrow \tau^+ Z' \nu_\tau$ is kinematically forbidden. However, the $g_{e\mu}$, $g_{\mu\mu}$ and $g_{\mu\tau}$ components can lead to a signal. If only $g_{\mu\tau}$ and/or $g_{\mu\mu}$ are nonzero, the new decay mode for the pion will be $\pi^+ \rightarrow \mu^+ Z' \nu$ which is suppressed due to the phase space suppression; *i.e.*, $(m_\pi - m_\mu)/(2m_\pi) \ll 1$. However with $g_{e\mu}$, we can have $\pi^+ \rightarrow e^+ Z' \nu$ and subsequently $Z' \rightarrow \nu_e \bar{\nu}_\mu$, $\nu_\mu \bar{\nu}_e$. Due to large background for ν_μ and $\bar{\nu}_\mu$, we should only rely on ν_e and $\bar{\nu}_e$ detection for reconstructing $g_{e\mu}$. If we allow both g_{ee} and $g_{e\mu}$ to be nonzero, a degeneracy between them will emerge. However, the combination of $g_{e\mu}$ and g_{ee} that the DUNE is sensitive to is different from the combination that the Kaon or pion decay experiments such as NA62 or PIENU can probe. Thus, in future, combining positive signals from the two types of experiments may help to break the degeneracy. DUNE can itself break the degeneracy between $g_{e\mu}$ and $g_{e\tau}$ by looking for the ν_τ signal.

V. SUMMARY AND DISCUSSION

We have studied the effects of the couplings of form $g_{\alpha\beta} \bar{\nu}_\alpha \gamma^\mu \nu_\beta Z'_\mu$ with $m_{Z'} \sim \text{few MeV} - \text{few } 10 \text{ MeV}$ at the near detector of DUNE. At the source, Z' can be produced via three body decay of the charged mesons, along with an electron (or a muon) and a neutrino. Subsequently, Z' decays into neutrino antineutrino pair before reaching the detector. The produced neutrinos can be detected at the near detector of DUNE.

The detection of ν_μ and $\bar{\nu}_\mu$ signal suffers from large background so we focus on g_{ee} and $g_{e\tau}$ elements that lead to ν_e , $\bar{\nu}_e$, $\bar{\nu}_\tau$ and ν_τ signals. Focusing only on the g_{ee} component, we find that with $\sim 10^{22}$ POT, the ND of DUNE can improve the bound on g_{ee} from NA62 for $m_{Z'} < 30$ MeV. For heavier Z' , the decay mode $\pi^+ \rightarrow Z' e^+ \nu$ will be suppressed by phase space so the NA62 experiment whose source is the K^+ decay sets a stronger bound. To extract information on $g_{e\tau}$ all the ν_e , $\bar{\nu}_e$, $\bar{\nu}_\tau$ and ν_τ signals can be invoked. As seen in Fig. 4, the bound that can be derived on $g_{e\tau}$ strongly depends on the efficiency of the ν_τ detection. Even with a 2 % efficiency, combining the ν_e , $\bar{\nu}_e$, ν_τ and $\bar{\nu}_\tau$ signals leads to a bound on $g_{e\tau}$ better than what can be derived from NA62 for entire $m_{Z'}$ range probed. Improving the efficiency up to 8 % (which considering the superb particle identification capabilities of DUNE sounds feasible) the bound can be significantly improved.

We also investigated the discovery potential of DUNE for nonzero g_{ee} and/or $g_{e\tau}$. We found that for a given true value of $m_{Z'}$, the ND of DUNE can set an upper bound on $m_{Z'}$; however, in the g_{ee} (or $g_{e\tau}$) and $m_{Z'}$ plane, the solution contours are elongated along $g_{e\alpha}/m_{Z'} = \text{cte}$ lines as $g_{e\alpha} \rightarrow 0$. This behavior originates from two facts: (1) for $m_{Z'} \rightarrow 0$, the longitudinal component of Z' leads to a $g^2/m_{Z'}^2$ behavior in the rate of $\pi^+ \rightarrow e^+ Z' \nu$; (2) for $m_{Z'} \rightarrow 0$, no special feature is expected.

While NA62 can only constrain $\sum_{\alpha \in \{e, \mu, \tau\}} |g_{e\alpha}|^2$, the ND of DUNE has the advantage of determining $g_{e\tau}$ and g_{ee} , separately by studying the ν_e and ν_τ signals. We have studied this possibility and the results are shown in Fig. 6.

The interactions that we are discussing can lead to non-standard neutrino neutrino interaction with immediate consequences for supernova neutrinos [4, 5]. The effective potential is given by the ratio $g^2/m_{Z'}^2$, which is a combination that can be well determined by DUNE ND. As demonstrated in Fig. 5, if $(g_{ee}/m_{Z'})^2$ or $(g_{e\tau}/m_{Z'})^2$ are of order of $4 \times 10^{-2} \text{ GeV}^{-2} \sim 4000 G_F$, the value of $g/m_{Z'}$ can be probed by DUNE ND. If a positive signal is found, it will have a distinct observable effect on supernova neutrinos so such information from DUNE ND is going to be an invaluable and unique input for analyzing supernova neutrinos.

Acknowledgments

We are grateful to Leo Bellantoni, Paul LeBrun and Laura Fields for providing us with information on the flux of charged mesons at the source of DUNE. We also thank A. Sousa, C. Eilkinson, A. Ereditato, S. Pascoli and B. Choudhary for useful discussions and encouragement. This project has received funding from the European Union’s Horizon 2020 research and innovation programme under the Marie Skłodowska-Curie grant agreement No. 674896

and No. 690575. YF is also grateful to the ICTP associate office and to IFIC, Valencia Univ. for warm and generous hospitality. P.B. thanks MPIK for their kind hospitality and support.

-
- [1] P. Ballett, T. Boschi and S. Pascoli, arXiv:1803.10824 [hep-ph].
 - [2] P. Coloma, B. A. Dobrescu, C. Frugiuele and R. Harnik, JHEP **1604** (2016) 047 doi:10.1007/JHEP04(2016)047 [arXiv:1512.03852 [hep-ph]]; B. Batell, P. deNiverville, D. McKeen, M. Pospelov and A. Ritz, Phys. Rev. D **90** (2014) no.11, 115014 doi:10.1103/PhysRevD.90.115014 [arXiv:1405.7049 [hep-ph]].
 - [3] L. G. van den Aarssen, T. Bringmann and C. Pfrommer, Phys. Rev. Lett. **109** (2012) 231301 [arXiv:1205.5809 [astro-ph.CO]].
 - [4] A. Das, A. Dighe and M. Sen, JCAP **1705** (2017) no.05, 051 doi:10.1088/1475-7516/2017/05/051 [arXiv:1705.00468 [hep-ph]].
 - [5] A. Dighe and M. Sen, Phys. Rev. D **97** (2018) no.4, 043011 doi:10.1103/PhysRevD.97.043011 [arXiv:1709.06858 [hep-ph]].
 - [6] P. B. Denton, Y. Farzan and I. M. Shoemaker, JHEP **1807** (2018) 037 doi:10.1007/JHEP07(2018)037 [arXiv:1804.03660 [hep-ph]]; J. Liao and D. Marfatia, Phys. Lett. B **775** (2017) 54 doi:10.1016/j.physletb.2017.10.046 [arXiv:1708.04255 [hep-ph]].
 - [7] Y. Farzan and J. Heeck, Phys. Rev. D **94** (2016) no.5, 053010 [arXiv:1607.07616 [hep-ph]].
 - [8] Y. Farzan and M. Tortola, Front. in Phys. **6** (2018) 10 doi:10.3389/fphy.2018.00010 [arXiv:1710.09360 [hep-ph]].
 - [9] P. Bakhti and Y. Farzan, Phys. Rev. D **95** (2017) no.9, 095008 doi:10.1103/PhysRevD.95.095008 [arXiv:1702.04187 [hep-ph]].
 - [10] E. Fernandez-Martinez, J. Hernandez-Garcia and J. Lopez-Pavon, JHEP **1608** (2016) 033 [arXiv:1605.08774 [hep-ph]].
 - [11] Leo Bellantoni, Laura Fields and Paul LeBrun, private correspondence.
 - [12] <http://home.fnal.gov/~ljf26/DUNE2015CDRFluxes/>
 - [13] M. D. Messier, UMI-99-23965.
 - [14] E. A. Paschos and J. Y. Yu, Phys. Rev. D **65** (2002) 033002 doi:10.1103/PhysRevD.65.033002 [hep-ph/0107261].
 - [15] C. Adams *et al.* [LBNE Collaboration], arXiv:1307.7335 [hep-ex].
 - [16] R. Acciarri *et al.* [DUNE Collaboration], arXiv:1512.06148 [physics.ins-det].
 - [17] J. Conrad, A. de Gouvea, S. Shalgar and J. Spitz, Phys. Rev. D **82** (2010) 093012 doi:10.1103/PhysRevD.82.093012 [arXiv:1008.2984 [hep-ph]].
 - [18] P. Astier *et al.* [NOMAD Collaboration], Phys. Lett. B **483** (2000) 387. doi:10.1016/S0370-2693(00)00611-0